ACS APPLIED MATERIALS & INTERFACES
Research Article
www.acsami.org

# Fabrication of Current Confinement Aperture Structure by Transforming a Conductive GaN:Si Epitaxial Layer into an Insulating GaOx Layer

Chia-Feng Lin,*[†] Wen-Che Lee,[†] Bing-Cheng Shieh,[†] Danti Chen,[‡] Dili Wang,[‡] and Jung Han*[‡]

[†]Department of Materials Science and Engineering, National Chung Hsing University, 250 Kuo Kuang Road, Taichung 402, Taiwan
[‡]Department of Electrical Engineering, Yale University, 15 Prospect Street, New Haven, Connecticut 06511, United States

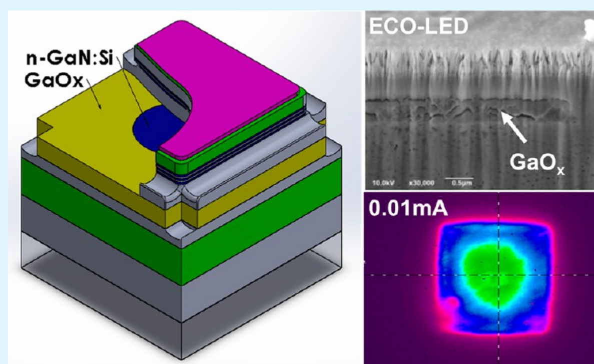


**ABSTRACT:** We report here a simple and robust process to convert embedded conductive GaN epilayers into insulating GaOx and demonstrate its efficacy in vertical current blocking and lateral current steering in a working LED device. The fabrication processes consist of laser scribing, electrochemical (EC) wet-etching, photoelectrochemical (PEC) oxidation, and thermal oxidization of a sacrificial $n^+$-GaN:Si layer. The conversion of GaN is made possible through an intermediate stage of porosification where the standard n-type GaN epilayers can be laterally and selectively anodized into a nanoporous (NP) texture while keeping the rest of the layers intact. The fibrous texture of NP GaN with an average wall thickness of less than 100 nm dramatically increases the surface-to-volume ratio and facilitates a rapid oxidation process of GaN into GaOX. The GaOX aperture was formed on the n-side of the LED between the active region and the n-type GaN layer. The wavelength blueshift phenomena of electroluminescence spectra is observed in the treated aperture-emission LED structure (441.5 nm) when compared to nontreated LED structure (443.7 nm) at 0.1 mA. The observation of aperture-confined electroluminescence from an InGaN LED structure suggests that the NP GaN based oxidation will play an enabling role in the design and fabrication of III-nitride photonic devices.

**KEYWORDS:** *nanoporous GaN, insulating GaOx, current confinement structure*

## 1. INTRODUCTION

As the performance of III-nitride blue-light-emitting diodes (LEDs) gradually reaches a state of saturation, attention has been given to alternative device configurations such as laser diodes[1] and vertical cavity surface emitting lasers (VCSEL).[2,3] In the development of infrared and red VCSELs in the 1990s, one of the landmark discoveries was the lateral oxidation of high Al-content Al(Ga)As epilayers[4,5] to create a current-confining aperture near the center of a microcavity. The lateral oxidation process converts Al(Ga)As into insulating aluminum oxide (AlOx) that blocks the parasitic current flow outside the microcavity and greatly improves the overlap of photonic modes with the injected carriers.[6,7]

Toward the realization of a similar building block for III-nitride photonic devices, several groups attempted to oxidize III-nitride layers. In the case of GaN, the oxidation processes are limited to less than 100 nm (dry oxidation) and revealed microcracks on thick oxide layers from the surface.[8] Regarding the use of ternary AlInN epilayers, Dorsaz[9] reported the electrochemical oxidation process of AlInN to form current apetures, even though the growth of AlInN remains a challenge and is not typically employed in LED structures.

Here, we report our process to convert embedded conductive GaN epilayers to $GaO_X$ as well as our results demonstrating the structure's ability to both block current vertically and steer current laterally in an LED device. The GaN porosfication step, is made possible through the selective anodization of n-type GaN, resulting in the n-type layer exclusively having a nanoporous (NP) structure. The nanoporous morphology is conducive to the transport of oxidizing agents in either liquid or vapor phases. In addition, the fibrous texture of NP GaN, which has significantly increased surface-to-volume ratio, serves as an advantage for the rapid oxidation that transforms GaN to $GaO_X$.

The insulating nature of converted $GaO_x$ is verified by Hall-effect and current−voltage measurements. X-ray diffraction indicates that the converted gallium oxide assumes a crystalline state of $Ga_2O_3$. The $GaO_x$ aperture forms on the n-side of the LED between the active region and the n-type GaN layer.

**Received:** September 3, 2014
**Accepted:** December 3, 2014
**Published:** December 3, 2014

 © 2014 American Chemical Society 

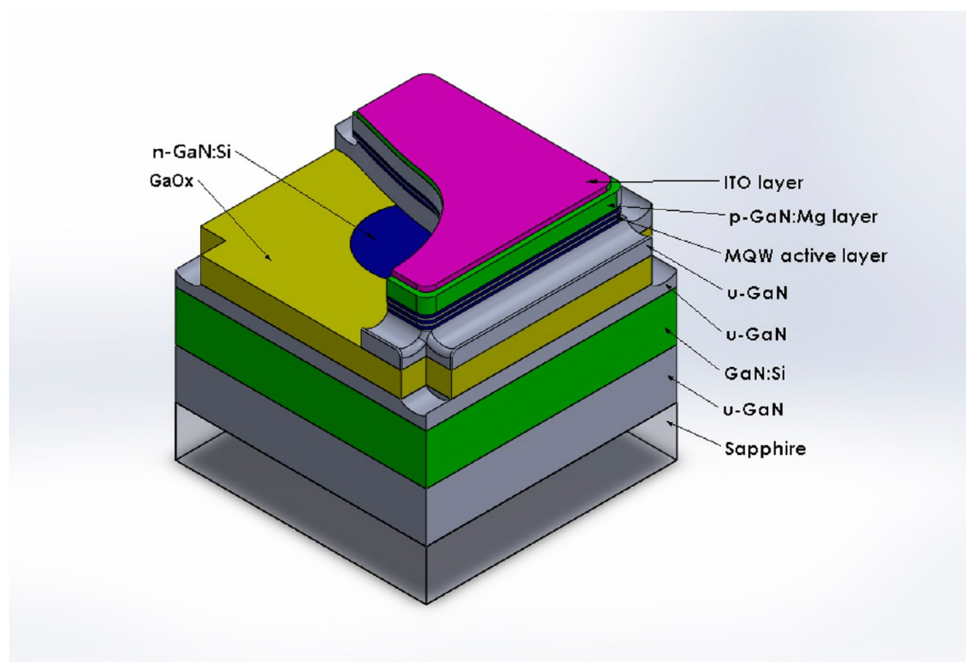


**Figure 1.** Schematic of the ECO-LED structure that fabricated through laser scribing process, EC lateral wet etching process, and oxidation process to current-confined aperture region.

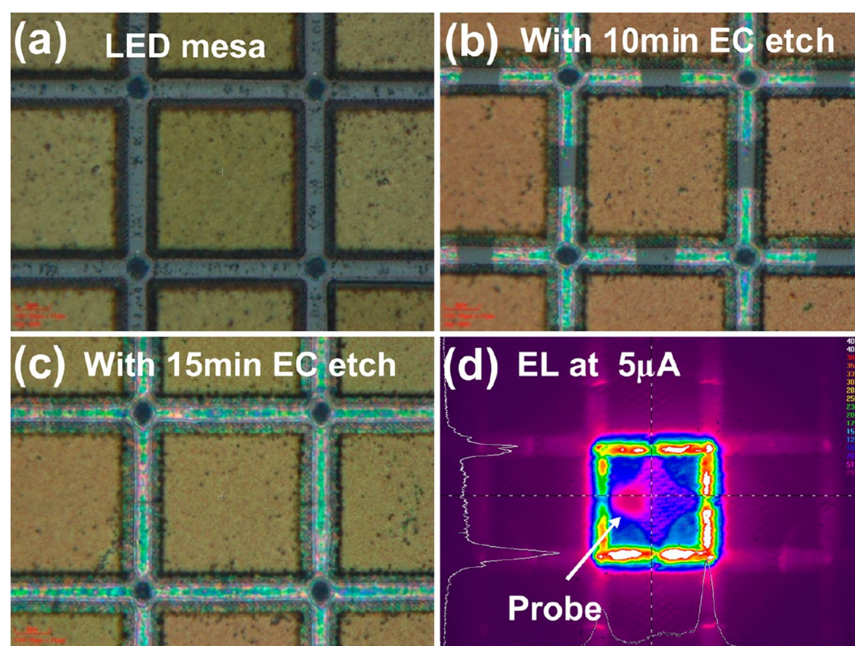


**Figure 2.** Microscopy images of the LED sample (a) without EC etching, (b) with 10 min etching time, and (c) with 15 min etching time were observed. (d) Star-shaped EL emission pattern was observed on the EC-treated mesa region at 0.005 mA injecting current.

## 2. EXPERIMENTAL DETAILS

InGaN-based LED structures were grown on a *c*-face (0001) 2 in. diameter patterned sapphire substrate through a metalorganic chemical vapor deposition system. These LED structures consists of a 30 nm thick GaN buffer layer, a 1.0 $\mu$m thick unintentionally doped GaN layer (u-GaN, background carrier concentration about $2 \times 10^{16}$ cm$^{-3}$), a 2.0 $\mu$m thick n-type GaN:Si layer ($1 \times 10^{18}$ cm$^{-3}$), a 0.1 $\mu$m thick u-GaN layer, a 0.43 $\mu$m thick heavily Si-doped n-type GaN layer ($5 \times 10^{18}$ cm$^{-3}$), a 0.1 $\mu$m thick u-GaN layer, 10 pairs of InGaN/GaN multiple quantum wells (MQWs) active layers, and a 0.12 $\mu$m thick magnesium-doped p-type GaN:Mg layer ($5 \times 10^{17}$cm$^{-3}$). Each active layer consists of a 30 Å thick InGaN-well layer and a 120 Å thick GaN-barrier layer for the InGaN/GaN MQW LED structure. A 400 nm-thick Indium Tin oxide (ITO) film and 50 nm Ti metal film were deposited on the p-GaN layer to serve as a transparent conductive layer and a protective layer, respectively, during the EC etching process. The dimensions of the LED chips are 40 × 40 $\mu$m$^2$ in size, and the mesa regions were defined by using a triple frequency ultraviolet Nd:$YVO_4$ (355 nm) laser for the front-side laser scribing process. The laser-scribing depth on the mesa region is about 0.3 $\mu$m, and the depth at the intersection region is about 0.6 $\mu$m to contact with the 0.43 $\mu$m thick n$^+$-GaN:Si sacrificial layer for the following EC-etching process. The laser scribing depth can be well-controlled through adjusting the laser pulse energy by using an optical variable

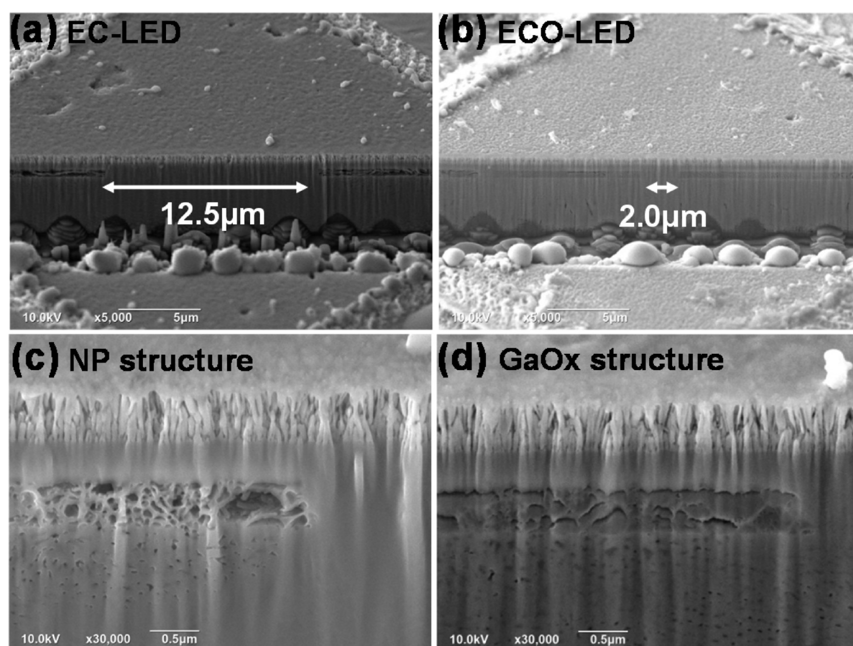


**Figure 3.** 45° tilted-view SEM micrographs of (a) the EC-LED and (b) the ECO-LED structure were observed. (c) Nanoporous GaN and (d) GaOx structures were observed close to the aperture region.

attenuator. All the samples were immersed in a 0.5 M oxalic acid solution for wet electrochemical (EC) etching with an external dc bias voltage of +18 V for 20 min. An external dc bias was fixed at a positive 18 V, applied on the bottom n-type GaN:Si layer surface as an anode contact, which is not immersed in the solution. A platinum electrode was used as the cathode for the wet etching process. The $n^+$-GaN layer can be etched to become a nanoporous GaN structure through the EC-etching process.[10,11] The samples were then oxidized through a photoelectrochemical (PEC) oxidation process at +20 V bias voltage and illuminated by a 400 W−Hg lamp in deionized water for 30 min.[12,13] The final result is the GaOx structure, transformed from the nanoporous GaN layer. The LED samples with the embedded GaOx layer were thermally treated at 650 °C by a hot wall furnace, in air ambient for 30 min. The Cr/Au (50 nm/2500 nm) metal layers, serving as ohmic contact layers, were deposited as n-type metal contacts. The LED with embedded the nanoporous GaN structure is defined as the electrochemically treated LED (EC-LED). The LED with the treated GaOx structure is defined as the ECO-LED. The nontreated LED structure is defined as the standard LED (ST-LED). The surface morphologies of all LED structures were observed through a scanning electron microscope (JEOL, JIB-4601F). The sheet resistivity and the carrier concentration of the samples were determined by the Hall effect measurements using the van der Pauw geometry with 0.5 T magnetic field. Ti/Al (5 nm/100 nm) metal bilayers with 500 $\mu$m diameter patterns were deposited on the corner of the 1 × 1 $cm^2$ in size samples, and were thermally annealed at 700 °C for 15 min to form the ohmic contact. The electroluminescence (EL) spectra and light output power were characterized through an optical spectrum analyzer, and the light intensity profiles were measured by a beam profiler.

## 3. RESULTS AND DISCUSSION

A schematic of the ECO-LED structure with a current confined aperture region fabricated through laser scribing, EC lateral wet etching, and oxidation processes is shown in Figure 1. The two-step laser scribing process forms a 40 $\mu$m grid with depth of 0.3 $\mu$m. Shown in Figure 2a is the microscopy image of the ST-LED. The lateral wet etching process occurred at the corner of the mesa region prepared by two step laser scribing processes. At the intersection of grid lines, the depth of the hole is 0.6 $\mu$m, which reaches the embedded $n^+$-GaN:Si sacrificial layer for the following EC etching process. The deep hole patterns can be observed in the OM images at the intersection of laser lines. The Ti/ITO bilayers (50 nm/400 nm) were deposited on the mesa region for the ohmic contact layer, and the top Ti metal layer has chemical stability to protect the top GaN:Mg layer during the EC etching process. After 10 min of EC etching at 18 V voltage bias, the lateral etching width is around 15um. In Figure 2b, the colorful image on the laser scribing line is caused by the light scattering process due the optical refractive index change in the EC-treated nanoporous GaN structure at $n^+$-GaN:Si sacrificial layer. After 15 min of EC etching, the two etching fronts, originating for the intersection hole, merge together as observed at the laser scribing region in Figure 2c. In Figure 2d, the star-shaped EL emission pattern is observed on the EC-treated mesa region under 0.005 mA injecting current condition.

The 45° tilted-view SEM micrographs of the EC-LED and the ECO-LED structure are shown in Figure 3. After the lateral wet etching process, the residual widths, as aperture regions, were measured to be 12.5 $\mu$m for the EC-LED and 2.0 $\mu$m for the ECO-LED as shown in Figure 3a, b, respectively. After the PEC oxidation process, the central aperture size was reduced from 12.5 to 2.0 $\mu$m. Figure 3c shows the nanoporous GaN structure at the lateral etched region on the $n^+$-GaN:Si sacrificial layer close to the central aperture region. After PEC oxidation process, the nanoporous GaN layer was transformed into the GaOx layer as shown in Figure 3d. After the oxidation process, the GaOx layer is formed and fills the space of the lateral etched region. Previously, many research groups have reported the thermal oxidation process on GaN nanowires. Li et al.[14] reported that the hexagonal GaN nanowires could be completely converted to $\beta$-$Ga_2O_3$ nanowires by annealing in air. Brendt et al.[15] reported the ammonolysis of $\beta$-$Ga_2O_3$ to $\alpha$-GaN and the oxidation of $\alpha$-GaN to $\beta$-$Ga_2O_3$. Tang et al.[16] reported the thermal oxidation of GaN nanowires in dry air. In this study, the EC-treated nonporous GaN structure is transformed

into the dense GaOx structure, which serves as a current confinement structure.

The X-ray diffraction curves of the ST-GaN, EC-GaN, and ECO-GaN structure are displayed in Figure 4. The ST-GaN structure consists a 1 $\mu$m-thick $n^+$-GaN:Si layer and 1 $\mu$m thick u-GaN layer on the sapphire substrate. After the EC etching process, the 1 $\mu$m thick $n^+$-GaN:Si layer was transformed into the nanoporous GaN:Si layer in the EC-GaN structure. Then, nanoporous GaN:Si layer was oxidized to become the GaOx layer in the ECO-GaN structure. Intense X-ray peaks were observed at 34.5° for the (0002) GaN and 41.8° for the (0006) $Al_2O_3$, respectively, in these three samples by using a 2$\theta$ rocking curve X-ray diffractometer. After the oxidation process, the peak of the GaOx layer was measured to be 38.4°. The enlarge X-ray curves of these three samples are shown in the inset plot in Figure 4. The small X-ray peak of the GaOx layer is observed in the ECO-GaN sample. The low X-ray intensity of the GaOx

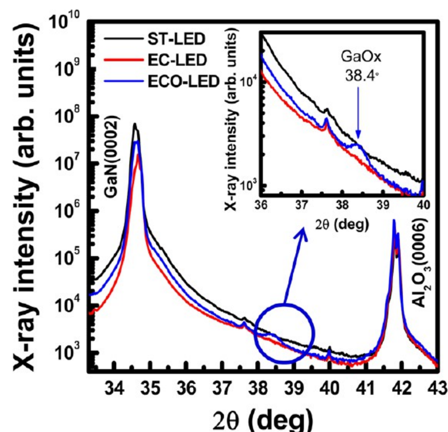


**Figure 4.** X-ray diffraction curve of the ST-GaN, EC-GaN, and ECO-GaN structure were measured. The inseted plot shows the enlarged X-ray curves of these three samples.

layer indicates that the crystalline quality of the GaOx is polycrystalline, formed through the low temperature thermal treatment. The electrical properties of these three samples were determined by using the Hall effect measurement at room temperature. The sheet resistivity and the carrier concentration were (42 Ω/□, 5.3 × $10^{18}$ $cm^{-3}$) and (270 Ω/s, 4.7 × $10^{17}$ $cm^{-3}$) for the ST-GaN and EC-GaN structure, respectively. After the EC etching process, the sheet resistivity of the nanoporous GaN structure (EC-GaN) increased compared to the nonetched $n^+$-GaN:Si layer (ST-LED). The carrier concentration of the nanoporous GaN:Si layer reduced to 4.7 × $10^{17}$ $cm^{-3}$ from the nonetched $n^+$-GaN:Si layer. The nanoporous GaN:Si layer still has the conductive property of the EC-GaN structure. However, no conductivity for the ECO-GaN structure could be measured using Hall effect measurement.

Figure 5 shows the light intensity profiles of the LED chips as analyzed by a beam profiler. In Figure 5a, uniform light-emission intensity is observed in the ST-LED at 0.04 mA injection current. The small light patterns in the ST-LED structure are caused by the light scattering effect at the bottom pattern sapphire substrate. After the EC lateral etching process at 18 V for 20 min, the rhombus-shaped emission pattern was observed in the emission image of the EC-LED structure as shown in Figure 5b. The lateral etching process occurred from the four intersections of laser lines at each mesa region, and the n+-GaN:Si layer had been etched to become the nanoporous structure surrounding the rhombus-shaped nontreated region. High EL emission intensity is observed on the whole mesa region of the EC-LED structure. In the EC-LED structure, the light emission intensity of the InGaN active layer with bottom nanoporous structure is higher than the central nonetched region. In the EC-LED structure, high EL emission intensity is observed surrounding the rhombus-shaped pattern, caused by the high light extraction efficiency on the EC-treated nanoporous GaN:Si structure. The bottom nanoporous GaN layer acts as an effective light scattering structure in the EC-

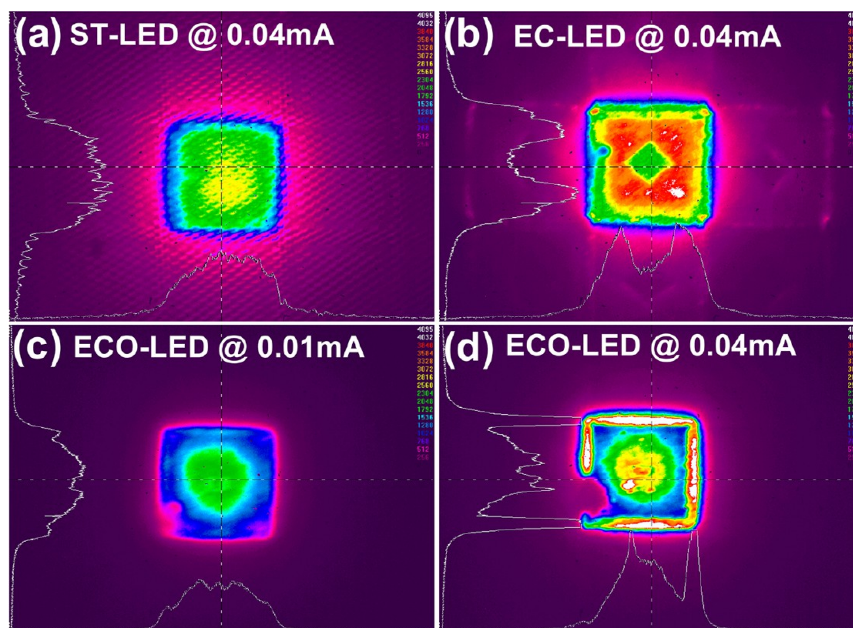


**Figure 5.** Light intensity profiles of (a) the ST-LED and (b) the EC-LED were analyzed by a beam profiler under 0.04 mA operation current. The light intensity profiles of the ECO-LED structure were measured at (c) 0.01 and (d) 0.04 mA operation currents.

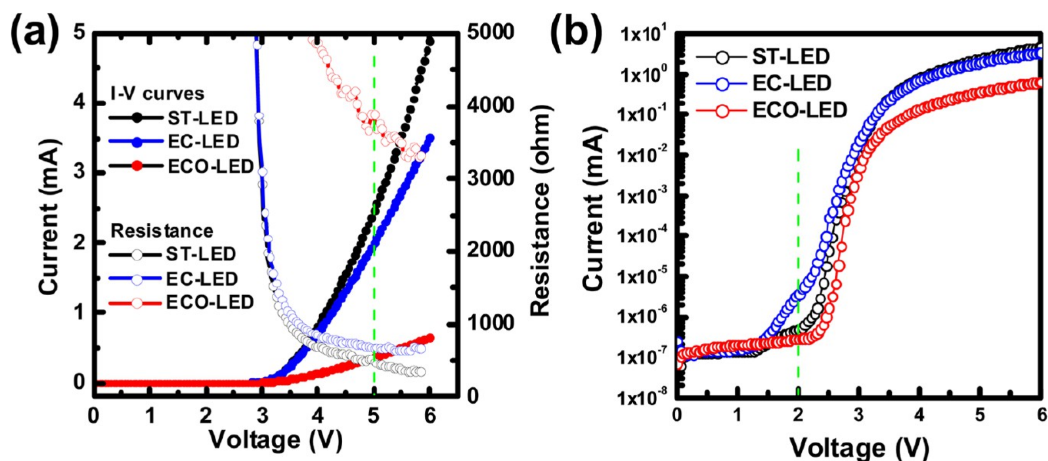


Figure 6. (a) Current and the series resistance as a function of the operation voltage were measured. (b) Current in logarithmic scale plot as a function of operating voltage was measured.

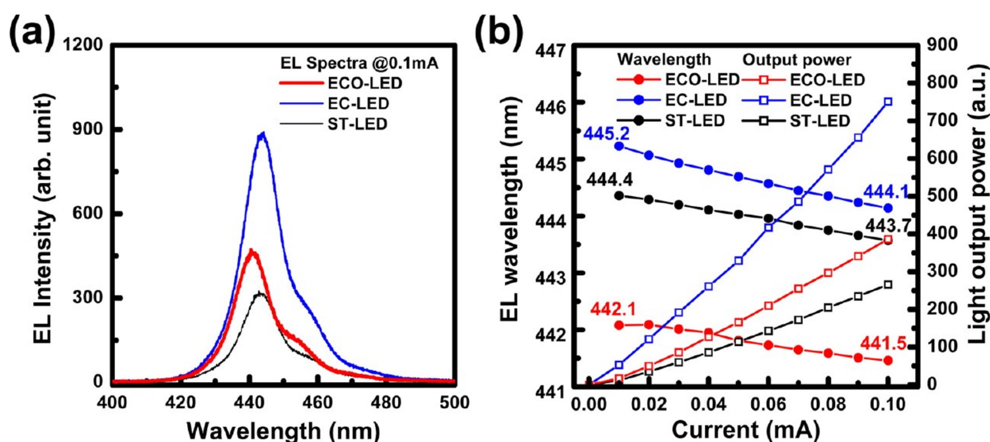


Figure 7. (a) EL spectra of ST-LED, EC-LED, and ECO-LED structures were measured at 0.1 mA operating current. (b) Peak wavelength of EL spectra and the light output power of all LED samples were measured by varying injection current from 0.01 to 0.1 mA.

LED structure. The oxidation process consists of PEC wet oxidation process and dry oxidation process in furnace at 650 °C. At low injection current in Figure 5c, the EL emission intensity is localized to the central mesa region indicating that the current did not flow into the mesa edge region with the bottom insulating GaOx layer. The dimensions of the central aperture region were reduced after the PEC oxidation process. In Figure 5c at 0.01 mA, the circle-shaped emission pattern is observed in the ECO-LED structure which indicates that the treated GaOx layer closed to the mesa sidewall became an insulating layer. A small aperture pattern is observed at the central mesa region, and the EL of the scattered light is detected surrounding the central aperture region. Figure 5d shows that by increasing the injection current to 0.04 mA, a high EL emission intensity is observed at the central aperture region. The EL light emitted from the center aperture region is extracted at the mesa edge region because of the low optical refractive index of the GaOx layer, which increases the light extraction efficiency.

The current and the series resistance as a function of the operation voltage were measured and are shown in Figure 6a. At 5 V operating voltage, the injection current and the series resistance were measured to be 2.47 mA/490ohm for the ST-LED, 2.01 mA/680 ohm for the EC-LED, and 0.37 mA/3890 ohm for the ECO-LED, respectively. After the EC etching process, the series resistance of the EC-LED slightly increased compared to the ST-LED indicating that the EC-treated nanoporous GaN is still a conductive material embedded in the LED structure. The series resistance of the ECO-LED structure was increased by reducing the current injection area, which indicates that the injecting current can be confined to the aperture region by the surrounding embedded-GaOx insulating layer. In Figure 6b, the current in logarithmic scale is plotted as a function of operating voltage was measured. At positive 2 V operation voltage below the turn-on threshold voltage, the injection current is measured at 0.5 $\mu$A for ST-LED, 3.8 $\mu$A for EC-LED, and 0.3 $\mu$A for ECO-LED, respectively. The slightly high forward leakage current is observed in EC-LED structure and is caused by some leakage process flowing through the embedded nanoporous GaN structure. In the ECO-LED structure, the injection current is confined to the central aperture region and the forward leakage current is suppressed by the surrounding insulating GaOx layer.

Figure 7a shows the EL spectra for ST-LED, EC-LED, and ECO-LED measured at 0.1 mA operating current. The peak wavelengths were measured as values of 443.7 nm for ST-LED, 444.1 nm for EC-LED, and 441.5 nm for ECO-LED, respectively. The highest EL emission intensity that is observed in the EC-LED structure is caused by the intense light scattering property and the electric conductivity of the

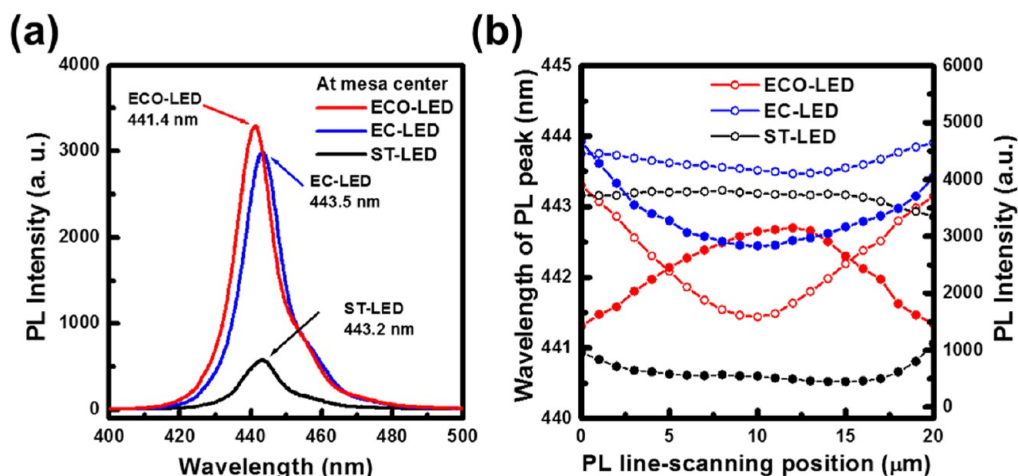


Figure 8. (a) Line-scan $\mu$-PL spectra of these three LED samples were measured at room temperature. (b) Peak wavelength and the peak intensity of the line-scan $\mu$-PL spectra were measured.

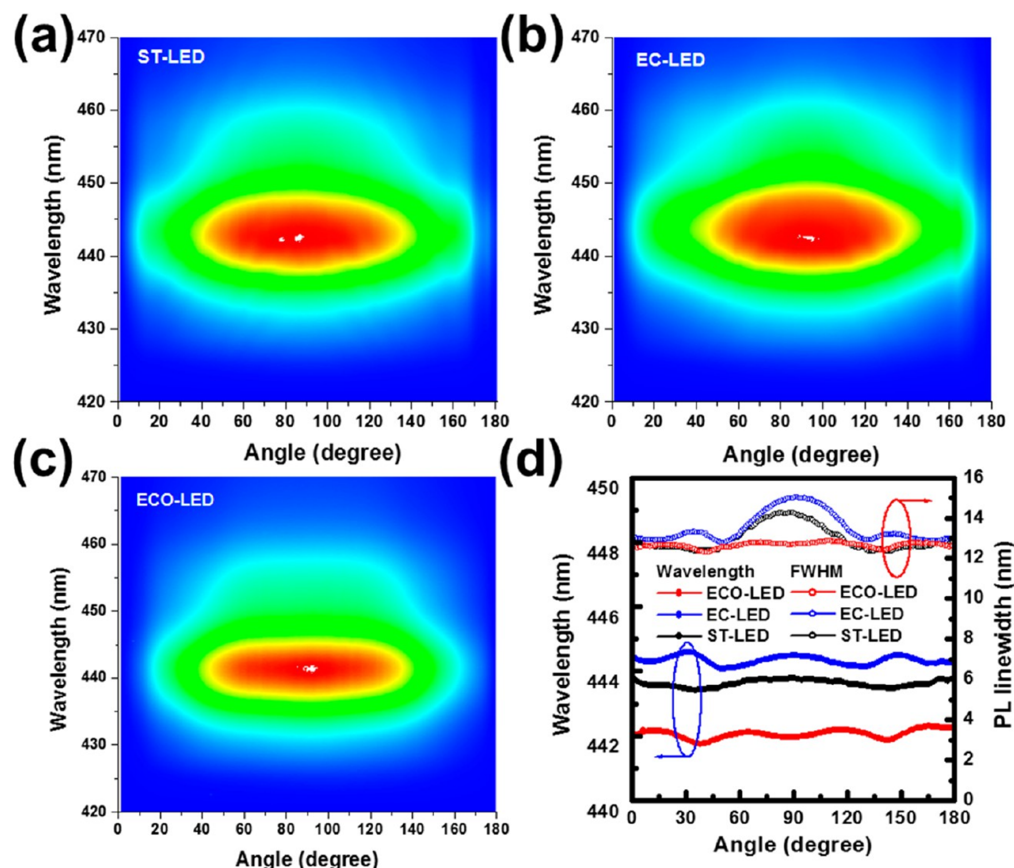


Figure 9. Normalized far-field emission spectra of LED structures are shown in (a) ST-LED, (b) EC-LED, and (c) ECO-LED structures by varying detected angles. (d) Peak emission wavelengths and the line-widths of the angle-resolved PL spectra were measured.

embedded EC-etched nanoporous structure. Part of the sacrificial $n^+$-GaN:Si layer had been etched to produce the nanoporous structure, but the residual part still has low resistance and high electric conductivity property. In Figure 7b, the peak wavelength of EL spectra and the light output power of all LED samples are measured by varying the injection current from 0.01 to 0.1 mA. At 0.01 mA/0.1 mA operating current, the peak EL emission wavelengths were measured at 444.4 nm/443.7 nm for the ST-LED, 445.2 nm/444.1 nm for the EC-LED, and 442.1 nm/441.5 nm for the ECO-LED structure, respectively. By increasing the injection current from 0.01 to 0.1 mA, the peak wavelength blueshift of the EL spectra were measured to be 0.7 nm for ST-LED, 1.1 nm for EC-LED, and 0.6 nm for ECO-LED structures, respectively. The peak wavelength blueshift phenomena are observed in these three LED structures are due to the band filling effect in the tilted band diagram of InGaN quantum well structures. The tilted InGaN band diagram is caused by compressive strain-induced piezoelectric field in InGaN active layer. The slightly longer emission wavelength and the larger wavelength blueshift

phenomenon are observed in the EC-LED structure compared to the nontreated ST-LED structure indicating that the piezoelectric field in the EC-LED structure slightly increased by the formation of the nanoporous GaN structure. Short emission wavelength and small wavelength blueshift phenomenon are measured in the ECO-LED structure because of the existence of the embedded GaOx layer. In the ECO-LED structure, the compressive strain in the InGaN active layer was slightly reduced after the formation of the bottom embedded GaOx layer. In Figure 7b, the light output power have 2.82 times and 1.45 times enhancements for the EC-LED and the ECO-LED, respectively, compared to the nontreated ST-LED structure. High current density in the aperture region and low refractive index of GaOx layer had increased the light output power in the ECO-LED structure.

Figure 8 shows the line scan u-PL emission spectra of the LED samples, measured at room temperature, using a 40 mW, 325 nm He−Cd lasers as an excitation laser source. The laser light was focused on the mesa surface with a 2 $\mu$m diameter laser spot. At the central mesa region, the peak emission wavelengths were 443.2 nm for the ST-LED, 443.5 nm for the EC-LED, and 441.4 nm for the ECO-LED structure, respectively, as shown in Figure 8a. The peak wavelength and the peak intensity of the line-scan $\mu$-PL spectra as a function of the PL line-scanning position are shown in Figure 8b, across the central mesa region. The PL peak wavelength of the EC-LED structure is slightly red-shifted compared to the ST-LED and could be due to the slightly increased compressive strain in the InGaN layer with embedded nanoporous structure. In the ECO-LED structure, the peak wavelengths have a blueshift phenomenon from the edge (443.1 nm) to the center (441.4 nm) of the mesa region. The PL intensity at the central mesa region is also higher than that of the edge region. Due to the formation of the oxidized nanoporous GaN layer, the compressive strain induced piezoelectric field in InGaN active layer is partially reduced at the central mesa region in the ECO-LED structure compared to ST-LED structure.

In Figure 9, the PL spectra were obtained by an angle-resolved PL measurement using a 405 nm excitation laser illuminated from the backside sapphire substrate and focused on the central mesa region. The laser light excites only the InGaN active region, and is not absorbed by the sapphire substrate, the n-type layer, or the p-type layer. The normalized emission spectra of LED structures are shown in Figure 9a for ST-LED, in Figure 9b for EC-LED, and in Figure 9c for ECO-LED structures by varying detecting angles. For the far-field radiation pattern measurement, the PL light emitted from the InGaN active layer is detected at the front-side of the LED chip. No obviously interference signals were observed in these three LED samples because the LED samples were grown on the patterned sapphire substrate. The peak emission wavelengths and the line-widths of the angle-resolved PL spectra are shown in Figure 9d. In the angular-resolved PL spectra, the slight oscillations of the peak emission wavelengths observed in all samples are caused by the minor interference effect in the LED epitaxial layers. The PL peak wavelengths of the EC-LED had a small redshift compared with the ST-LED structure. After the oxidation process, the ECO-LED structure with embedded GaOx layer has shorter PL emission wavelengths and stable PL line-widths compared to the ST-LED structure. In the ECO-LED structure, the peak wavelength blueshift phenomena observed in the EL and the PL spectra indicates that the strain-induced piezoelectric effect in the InGaN active layer were partially released by the formation of the bottom GaOx layer.

## 4. CONCLUSION

In conclusion, InGaN LED structure with the current confined aperture structure was fabricated through the lateral oxidation process on the inserted $n^+$-GaN:Si layer between the InGaN active layer and the n-type GaN:Si layer. High light extraction efficiency is observed in the EC-LED structure that had the embedded nanoporous GaN structure. The nanoporous GaN structure was transformed into the insulating GaOx structure through the oxidation processes. The injection current in the ECO-LED was confined into an n-type aperture structure by surrounding embedded-GaOx structure. The embedded GaOx structure in the ECO-LED structure acted as an effective light scattering structure and a current confinement structure that has the potential for nitride-based VCSEL device applications.

## ■ AUTHOR INFORMATION


### Corresponding Authors

*E-mail: cflin@dragon.nchu.edu.tw.

*E-mail: jung.han@yale.edu.


### Notes

The authors declare no competing financial interest.

## ■ ACKNOWLEDGMENTS


The authors gratefully acknowledge the financial support for this research by the National Science Council of Taiwan under Grants 102-22 18-E-005-010-MY3 and 102-2221-E-005-067. Chia-Feng Lin and Jung Han contributed equally to this work.


## ■ REFERENCES


(1) Nakamura, S. The Roles of Structural Imperfections in InGaN-Based Blue Light-Emitting Diodes and Laser Diodes. *Science* **1998**, *281*, 956−961.

(2) Someya, T.; Werner, R.; Forchel, A.; Catalano, M.; Cingolani, R.; Arakawa, Y. Room Temperature Lasing at Blue Wavelengths in Gallium Nitride Microcavities. *Science* **1999**, *285*, 1905−1906.

(3) Butté, R.; Feltin, E.; Dorsaz, J.; Christmann, G.; Carlin, J. F.; Grandjean, N.; Ilegems, M. Recent Progress in the Growth of Highly Reflective Nitride-Based Distributed Bragg Reflectors and Their Use in Microcavities. *Jpn. J. Appl. Phys.* **2005**, *44*, 7207−7216.

(4) Yang, G. M.; MacDougal, M. H.; Dapkus, P. D. Ultralow Threshold Current Vertical-cavity Surface-emitting Lasers Obtained with Selective Oxidation. *Electron. Lett.* **1995**, *31*, 886−888.

(5) Bissessur, H. K.; Koyama, F.; Iga, K. Modeling of Oxide-confined Vertical-cavity Surface-Emitting Lasers. *IEEE J. Sel. Top. Quantum Electron.* **1997**, *3*, 344−352.

(6) MacDougal, M. H.; Dapkus, P. D.; Bond, A. E.; Lin, C.-K.; Geske, J. Design and Fabrication VCSEL's with AlxOy −GaAs DBR's. *IEEE J. Sel. Top. Quantum Electron.* **1997**, *3*, 905−915.

(7) Maranowski, S. A.; Sugg, A. R.; Chen, E. I.; Holonyak, N., Jr. Native Oxide Top- and Bottom-Confined Narrow Stripe *p-n* $Al_yGa_{1-y}As$-GaAs-$In_xGa_{1-x}As$ Quantum Well Heterostructure laser. *Appl. Phys. Lett.* **1993**, *63*, 1660−1662.

(8) Peng, L. H.; Liao, C. H.; Hsu, Y. C.; Jong, C. S.; Huang, C. N.; Ho, J. K.; Chiu, C. C.; Chen, C. Y. Photoenhanced Wet Oxidation of Gallium Nitride. *Appl. Phys. Lett.* **2000**, *76*, 511−513.

(9) Dorsaz, J.; Bühlmann, H. J.; Carlin, J. F.; Grandjean, N.; Ilegems, M. Selective Oxidation of AlInN Layers for Current Confinement in III−nitride Devices. *Appl. Phys. Lett.* **2005**, *87*, 072102.

(10) Park, J.; Song, K. M.; Jeon, S. R.; Baek, J. H.; Ryu, S. W. Doping Selective Lateral Electrochemical Etching of GaN for Chemical Lift-off. *Appl. Phys. Lett.* **2009**, *94*, 221907.

(11) Zhang, Y.; Ryu, S. W.; Yerino, C.; Leung, B.; Sun, Q.; Song, Q.; Cao, H.; Han, J. A Conductivity-based Selective Etching for Next Generation GaN Devices. *Phys. Status Solidi B* **2010**, *247*, 1713−1716.
(12) Lin, C. F.; Yang, Z. J.; Zheng, J. H.; Dai, J. J. Enhanced Light Output in Nitride-based Light-emitting Diodes by Roughening the Mesa Sidewall. *IEEE Photonics Technol. Lett.* **2005**, *17*, 2038−2040.
(13) Lin, C. F.; Chen, K. T.; Huang, K. P. Blue Light-Emitting Diodes with an Embedded Native Gallium Oxide Pattern Structure. *IEEE Electron Device Lett.* **2010**, *31*, 1431−1433.
(14) Li, J.; An, L.; Lu, C.; Liu, J. Conversion between Hexagonal GaN and $\beta$-$Ga_2O_3$ Nanowires and Their Electrical Transport Properties. *Nano Lett.* **2006**, *6*, 148−152.
(15) Brendt, J.; Samuelis, D.; Weirich, T. E.; Martin, M. An in SituXAS Investigation of the Kinetics of the Ammonolysis of $Ga_2O_3$ and the Oxidation of GaN. *Phys. Chem. Chem. Phys.* **2009**, *11*, 3127−3137.
(16) Tang, C.; Bando, Y.; Liu, Z. Thermal Oxidation of Gallium Nitride Nanowires. *Appl. Phys. Lett.* **2003**, *83*, 3177−3179.